IJRCS

International Journal of Robotics and Control Systems
Vol. 5, No. 2, 2025, pp. 881-901
ISSN 2775-2658
http://pubs2.ascee.org/index.php/ijrcs

ASCEE

Fuzzy Dynamic Feedback Linearization for Efficient Mobile Robot Trajectory Tracking and Obstacle Avoidance in Autonomous Navigation

Souhaib Louda [a,1,*], Nora Karkar [a,2], Fateh Seghir [a,3], Oussama Boutalbi [a,b,4]

[a] LSI Laboratory, Electronics Department, Ferhat Abbas Setif 1 University, Setif, 19000, Algeria
[b] Institute of Science, Center of Morsli Abdellah Tipaza University, Tipaza, 42000, Algeria
[1] souhaib.louda@univ-setif.dz; [2] nora.karkar@univ-setif.dz; [3] fateh.seghir@univ-setif.dz;
[4] botalbioussama@gmail.com
[*] Corresponding Author

ARTICLE INFO

Article History
Received January 10, 2025
Revised February 11, 2025
Accepted March 06, 2025

Keywords
Trajectory Tracking;
Obstacle Avoidance;
Fuzzy Logic Controller;
Dynamic Feedback Linearization;
Mobile Robots;
Robot Operating System

ABSTRACT

Mobile robots are increasingly used in various applications that require precise trajectory tracking and efficient obstacle avoidance. Dynamic Feedback Linearization (DFL) is powerful method, however, it's has limitations such as increased computational requirements, model dependency, inability to avoid obstacles, and reduced robustness. In this paper, we address the challenges of trajectory tracking and obstacle avoidance for non-holonomic mobile robots in certain static environments subjected to the challenge of the robot to follow the reference trajectory accurately while avoiding the known obstacle in the trajectory of the robot by switching the two behaviors. The proposed scheme leverages the adaptive performance control to minimize the error between the reference and actual trajectories and avoid the static obstacle successfully. Firstly, the Dynamic Feedback Linearization (DFL) concept is used to develop an efficient tracking control system. Secondly, a Fuzzy Logic Controller (FLC) is used to avoid obstacles in the reference trajectory of the robot . Finally, the simulations are conducted using MATLAB software and the TurtleBot2 mobile robot within the 3D Gazebo simulator. According to the simulation results, the proposed approach cuts tracking accuracy and obstacle avoidance success rate by 93% and 95%, respectively. Additionally, experimental validation is carried out with the Adapt Mobilerobots Pioneer-3DX mobile robot, the results obtained from the Robot Operating System (ROS) prove the efficacy of the proposed approach for efficiency and precision.

This is an open access article under the CC-BY-SA license.

1. Introduction

Differential wheeled mobile robots (DWMRs) motion control has recently been the focus of several study areas [1]–[6]. Specifically, exact tracking control and safe navigation tasks have received special attention [7]–[10].

The tracking control problem in mobile robotics involves designing a control strategy that allows a robot to follow a predefined path or trajectory accurately [11]–[13]. The goal is to reduce the error between the actual trajectory of the robot and the desired trajectory during the tracking task. Effective tracking requires continuous adjustments based on the robot's current pose, speed, and heading to ensure that it aligns with the planned path.

Safe navigation tasks focus on ensuring that a mobile robot can reach its destination while avoiding collisions and maintaining safety restrictions [14], [15], [19]. This includes obstacle detection and avoidance, real-time path adjustments, and adherence to safe speeds and distances from objects in static and dynamic environments. For robust safe navigation, the robot uses sensors such as Lidar, cameras, and sonar to perceive its surroundings and make decisions that keep it clear of obstacles, accounting for its shape, velocity, and dynamic constraints.

The non-holonomic type kinematic constraints are connected to these nonintegrable systems and have inspired the creation of extremely non-linear control methods [21].

This type of robot has constraints that reduce the range of possible solutions to both trajectory planning and control design problems. Essentially, it suggests that the robot is a member of the class of systems that faces a lot of challenges the first one is that it cannot have a smooth time-invariant controller to stabilize it Secondly, it cannot accept the growth of special controllers developed for the tracking to solve the problem of the set point control and vice versa. It is essential to pay special attention to this phase when designing desired reference trajectories to guarantee feasible task planning [22].

There are various efficient approaches for addressing the regulation and trajectory tracking issues associated with mobile robots. such as sliding mode control [23]–[25] , backstepping [26], Fuzzy logic controller [27], Time-varying controllers based on Lyapunov stability method [28], [29], An overview of the elementary methods used for trajectory tracking and feedback motion control is presented in [30],

The most important approach is that of dynamic feedback linearization, which is an excellent design tool applicable to open-loop control system design (trajectory planning) [31]. The main problems of trajectory tracking and set-point regulation are presented in [32]–[34], A significant attribute of feedback linearizable systems is differential flatness [22], [35], [36], The notion of controllability is intrinsically connected to the structural feature of controllability. As an expansion of Brunovsky's work, this method of study has proven to be a powerful tool for the analysis and design of open-loop and stabilizing feedback tracking control for nonlinear finite-dimensional systems. It can be applied to outputs for linear controlled systems to non-linear. [37]–[42], The flatness property was employed for the regulation of continuous non-linear systems, which demonstrated favorable performance in terms of trajectory tracking [43], [53].

The obstacle avoidance task [44] is an essential task to ensure the mobile robot moves safely and avoids collision with obstacles. There are many techniques such as reinforcement learning [45], neural network [46], Artificial Potential Field (APF) [47], [20], Dynamic Window Approach (DWA) [48], Time Elastic Band (TEB) [49], and Vector Field Histogram (VFH) [50]...

The Fuzzy logic Controller is a famous controller in obstacle avoidance proposed by mathematician Lotfi Zadeh in 1965, We choose it because it is easy to implement and very efficient in any type of environment [51], [59].

There have been relatively perfect solutions to trajectory following with an obstacle avoidance hybrid approach for wheeled mobile robots. In the literature related to the mobile robot hybrid approach, Trakas [55] proposes an adaptive performance control to dynamically adjust the user-defined output performance specifications, ensuring compliance with input and safety constraints. subjected to diamond-shaped velocity constraints. Zheng [56] proposes an dual-loop trajectory tracking control and the improved artificial potential field method, the autonomous obstacle avoidance and trajectory planning scheme of the mobile robot is designed, and closed-loop stability verification and analysis are conducted on the overall control system. Sezer [57] proposes a new path tracker method for autonomous robots by re-designing a classical obstacle avoidance algorithm, "Follow the Gap Method (FGM)", To use the FGM as a dynamic tracker, the proposed methodology is borrowing the "Look Ahead Distance" (LAD) from geometric path tracking methods and adapting it to the local planner.

Abdelwahab [58] proposes a Z-number-based Fuzzy Logic Control (Z-FLC) approach for trajectory tracking of DWMR's. This method uniquely encodes constraints and reliability in multi-input, multi-output fuzzy rules while relying only on instantaneous measurements of distance and orientation gaps.

Based on this above discussion, a novel hybrid approach called (F-DFL) is proposed in this paper. In this approach, a dynamic feedback linearization (FDL) used in trajectory tracking is combined with a fuzzy logic controller (FLC) to avoid any static obstacles in the predefined path. This hybrid approach allows for guiding the robot moves safely during the process.

To achieve trajectory tracking control and prevent collisions with static obstacles, The main contributions of this work are as follows:

- A novel hybrid approach in mobile robot navigation, called Fuzzy-Dynamic Feedback linearization, is proposed to achieve trajectory tracking and obstacle avoidance tasks simultaneously
- Implementation of a fuzzy-dynamic feedback linearization (FDFL) technique using ROS MATLAB and testing our approach in ROS Gazebo simulator in real time, the results obtained in MATLAB and Gazebo are very similar which considered kinematics constrained of differential mobile robot.
- Experimental validation of the proposed approach was conducted in real time using the Robot Operating System (ROS) with a master-slave connection. A powerful high-level PC handled processing tasks, while a low-level laptop PC managed control tasks, connected wireless between them.

This paper is organized as follows: In Section. 2 The mathematical modeling and problem formulation of the mobile robot are presented; In Section. 3, the solution to the problem is proposed; In Section. 4 and Section. 5 simulation and experimental results are discussed, and the final section provides a concise conclusion along with suggestions for future work.

2. System Modeling And Problem Formulation

2.1. Kinematic Model of the Mobile Robot

A simplified schematic of a differentially driven wheeled mobile robot is depicted in Fig. 1, where $(OXgYg)$ is a fixed inertial frame, (OX_lY_l) is an attached frame to the mobile platform, L represents the distance between the right and left wheels of the robot, and r is the radius of both wheels.

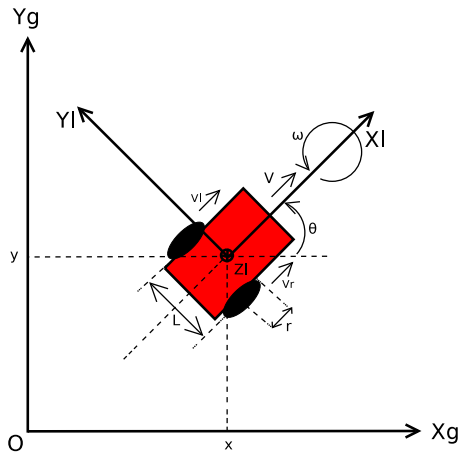

Fig. 1. Kinematic model of mobile robot

The configuration of the robot is characterized by its position (x, y) in the plane and its orientation θ relative to the global reference frame $(OXgYg)$. The robot's state can be represented by the vector $\mathbf{q} = [x \;\; y \;\; \theta]^T$,where $([.]^T$ denotes the transpose operator).

Let v_L and v_R be the linear velocities of the left and right wheels, respectively. The robot's linear velocity v and angular velocity ω can be derived from the wheel velocities as follows:

$$\begin{aligned} v &= \frac{v_R + v_L}{2} \\ \omega &= \frac{v_R - v_L}{L} \end{aligned} \tag{1}$$

The differential kinematic equations describing the motion of the robot are expressed as follows:

$$\begin{aligned} \dot{x} &= v\cos\theta \\ \dot{y} &= v\sin\theta \\ \dot{\theta} &= \omega \end{aligned} \tag{2}$$

Substituting the expressions for v and ω, we get:

$$\begin{aligned} \dot{x} &= \frac{v_R + v_L}{2}\cos\theta \\ \dot{y} &= \frac{v_R + v_L}{2}\sin\theta \\ \dot{\theta} &= \frac{v_R - v_L}{L} \end{aligned} \tag{3}$$

These equations form the basis for controlling and simulating the motion of differential drive mobile robots.

$$\dot{y}\cos\theta - \dot{x}\sin\theta = 0 \tag{4}$$

$$\dot{x}\cos\theta + \dot{y}\sin\theta + \frac{l}{2}\dot{\theta} - v_R = 0 \tag{5}$$

$$\dot{x}\cos\theta + \dot{y}\sin\theta - \frac{l}{2}\dot{\theta} - v_L = 0 \tag{6}$$

In (4)–(6) can be used to model the motion of a differential drive robot, The three equations ensure that the lateral velocity of the robot is zero, which means it is always moving along the x_b axis, and that the wheels of robot roll without slipping.

2.2. Problem Formulation

The goal is to design a control strategy for a mobile robot to achieve both accurate trajectory tracking and obstacle avoidance. Given a desired smooth trajectory $(x_d(t), y_d(t))$, the approach must:

- **Track the desired trajectory**: Minimize the error between the robot's current position $(x(t), y(t))$ and the desired trajectory, ensuring smooth and precise tracking.
- **Avoid Obstacles using Fuzzy Control**: Implement a fuzzy logic controller to dynamically adjust the robot's motion and avoid static obstacles, maintaining a safe distance while still following the trajectory.

3. The Proposed Approach

A general overview of the proposed solution in this paper is depicted in Fig. 2. It is composed of three main blocks. The tracking control block is based on Dynamic Feedback Linearization (DFL) and the obstacle avoidance block based Fuzzy Logic Controller (FLC) is devoted to ensuring the robot does not collide with any obstacle in a predefined trajectory then The fusion block combines the two behaviours for accomplish the task.

The Fig. 2 presents a hybrid control architecture for a differential wheeled mobile robot (DWMR, TurtleBot2), incorporating a trajectory tracking controller (DFL, Dynamic Feedback Linearization)

alongside an obstacle avoidance controller (FLC, Fuzzy Logic Controller). The DFL receives the error between the desired and actual trajectory (e_x, e_y, e_θ) and generates the control commands (v_t, w_t) to ensure precise tracking. In parallel, the FLC utilizes obstacle distance data measured via the odometry in Odometry ROS message in /odom topic to produce avoidance commands (v_a, w_a) to prevent collisions. These two outputs are combined in a fusion module, which generates the final velocity commands (v, w), ensuring a balance between trajectory tracking and obstacle avoidance. The final commands are then published to the /cmd_vel topic to control the TurtleBot2, while the actual position (x,y,θ) is updated using odometry data from the /odom topic. This approach enables effective autonomous navigation by combining precise trajectory tracking with static obstacle avoidance.

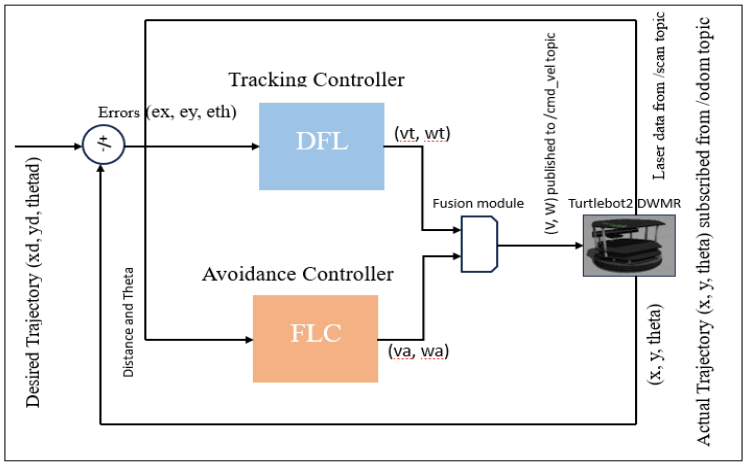

Fig. 2. General overview of the proposed solution

3.1. Trajectory Tracking using Dynamic Feedback Linearization

Using the fact that the vector of Cartesian coordinates of a unicycle robot model in (2) are flat outputs, a feedback linearizing control law can be defined as :

$$\begin{aligned} u_1 &= \ddot{x}_d + k_{p_1}\left(x_d - x\right) + k_{d1}\left(\dot{x}_d - \dot{x}\right) \\ u_2 &= \ddot{y}_d + k_{p_2}\left(y_d - y\right) + k_{d2}\left(\dot{y}_d - \dot{y}\right) \end{aligned} \tag{7}$$

Where

$$\begin{aligned} \xi &= u_1 * \cos\theta + u_2 * \sin\theta \\ v &= \int \xi \, dt \\ \omega &= \frac{u_2 * \cos\theta - u_1 * \sin\theta}{v} \end{aligned} \tag{8}$$

$$\ddot{F} = \begin{bmatrix} \ddot{x} \\ \ddot{y} \end{bmatrix} = \begin{bmatrix} \cos(\theta) & -v\sin(\theta) \\ \sin(\theta) & v\cos(\theta) \end{bmatrix} \begin{bmatrix} \xi \\ \omega \end{bmatrix} \tag{9}$$

Where (x_d, y_d) indicates the desired trajectory, and $k_{p_1}, k_{p_2}, k_{d_1}, k_{d_2}$ represents the constant conficients, θ represent the orientation of the robot, v and ω are the linear and angular velocities of the robot.

The selection of control techniques plays a critical role in the effectiveness and robustness of autonomous mobile robots in static environments. In this study, Dynamic Feedback Linearization (DFL) was chosen for trajectory tracking due to its ability to linearize the robot's inherently nonlinear dynamics, ensuring precise and efficient path-following in real time. In contrast, the Fuzzy Logic

Controller (FLC) was selected for obstacle avoidance because of its flexibility, robustness to uncertainty, and capability to handle complex and dynamic environments. Together, these controllers, as defined in (8) and (24), offer a powerful and complementary solution for mobile robot navigation. They enable the robot to track its trajectory accurately while effectively avoiding obstacles.

3.2. Obstacle Avoidance based Fuzzy Logic Controller

The second objective of the proposed solution is to ensure the robot effectively avoids obstacles encountered along its predefined trajectory.

As seen in Fig. 3, the process of constructing a fuzzy controller [16], which serves as the foundational element of fuzzy control, encompasses four fundamental stages: input fuzzification, construction of fuzzy control rules, fuzzy inference, and defuzzification. Among these, the construction of fuzzy control rules is of the utmost importance.

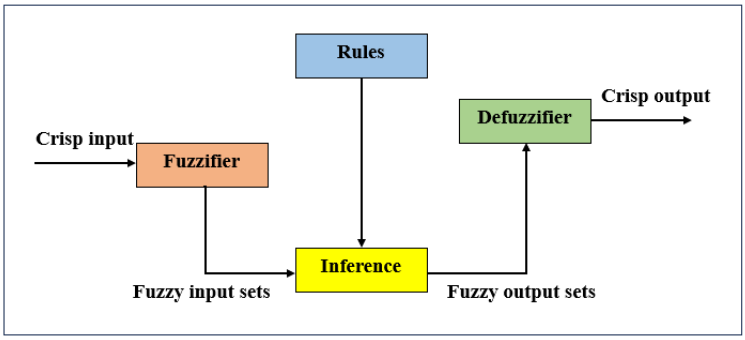

Fig. 3. Fuzzy logic controller structure

The fuzzy controller developed is designed with two fuzzy input variables and one fuzzy output variable. The inputs to the fuzzy controller are: Dobst represents the nearest distance between the robot and the obstacle, and Thetaobs is the angle between the robot and the obstacle. The output of the fuzzy controller is the flatness parameter, F.

In the fuzzy controller, the input and output variables are defined by continuous theoretical domains, with triangular and trapezoidal membership functions employed as the affiliation functions are shown in Fig. 4. The input variable Dobs is constrained to the interval [0, 2], and its associated fuzzy sets are designated as ”Close” and ”Far,” which correspond to the near and far distances, respectively. Furthermore, the input variable Thetaobs is set to [-4, 4], and the corresponding fuzzy sets, ”Negative,” ”Zero,” and ”Positive,” represent the angle error between the robot and the obstacle.

The output of variable variable F is in the universe of discourse [0, 1]. Accordingly, the fuzzy set is stipulated as ”Little,” ”More,” and ”Lots,” which correspond to small changing, medium changing, and high changing, respectively. The affiliation function graph for the output variable is depicted in Fig. 4.

The underlying principle of a fuzzy approach entails a set of fuzzy rules derived from their affiliation function. The application of these rules involves exactly mapping values in an argument’s domain to various fuzzy subsets. The substitution of fuzzy variable values allows for the attainment of fuzzy control. The Table. 1 The table presents a fuzzy rules table implemented inside the fuzzy controller. Based on the receiving data of input distance and angle, the controller decides the output value of F for tracking and avoidance tasks.

After collecting the output variable, the fuzzy vector is created using the Mamdani-type fuzzy inference method. Subsequently, accurate output control values are determined using defuzzification utilising the centre of gravity method. This allows the coefficient F of the fusion function to be determined.

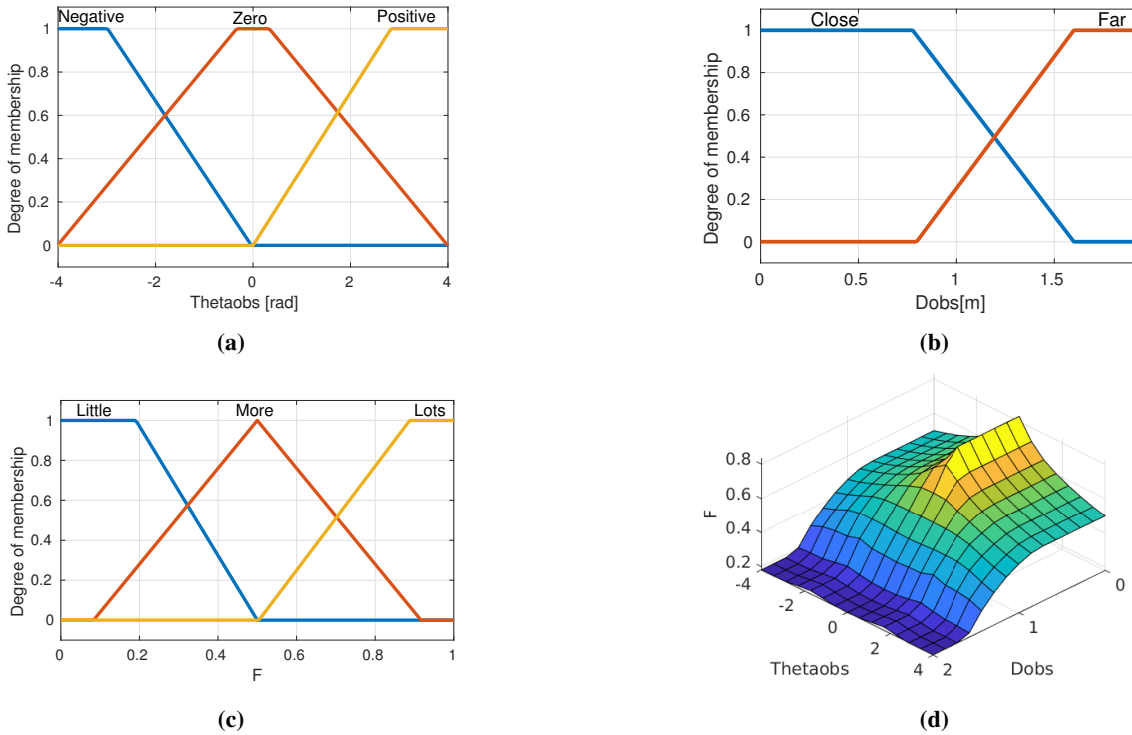

Fig. 4. Membership functions and fuzzy surfaces for input and output variables: (a) Input variable *thetaObs* and its membership function, (b) Input variable *distObs* and its membership function, (c) Output variable *F* and its membership function, (d) Three-dimensional fuzzy surface graph

Table 1. Fuzzy rule bases for F

Rule	Inputs		Output
	distObs	thetaObs	F
1	Close	Negative	More
2	Close	Zero	Lots
3	Close	Positive	More
4	Far	Negative	Little
5	Far	Zero	Little
6	Far	Positive	Little

3.3. Fusion Process

In this process, we use a switching technique between tracking and avoidance control based on the value of F as shown in (10) and (11), Here v and ω represent final linear and angular velocities, respectively, which are sent as command velocities for the motion control of the mobile robot. Specifically, v_{tr}, ω_{tr} denote the actual linear and angular velocities for the tracking task, while v_{av}, ω_{av} refer to the actual linear and angular velocities for the avoidance task.

$$v = (1 - F)v_{tr} + Fv_{av} \tag{10}$$

$$w = (1 - F)w_{tr} + Fw_{av} \tag{11}$$

The value of F in (10) and (11), is determined as the output of the Fuzzy Logic Controller (FLC). This value ranges between [0, 1] and increases when the distance to a static obstacle falls below the safe distance, prioritizing obstacle avoidance. Conversely, F decreases when the robot is farther from obstacles, prioritizing trajectory tracking and ensuring safe navigation during the task. A flowchart shown in Fig. 5 describes the combination of DFL with FLC for trajectory tracking and obstacle avoidance.

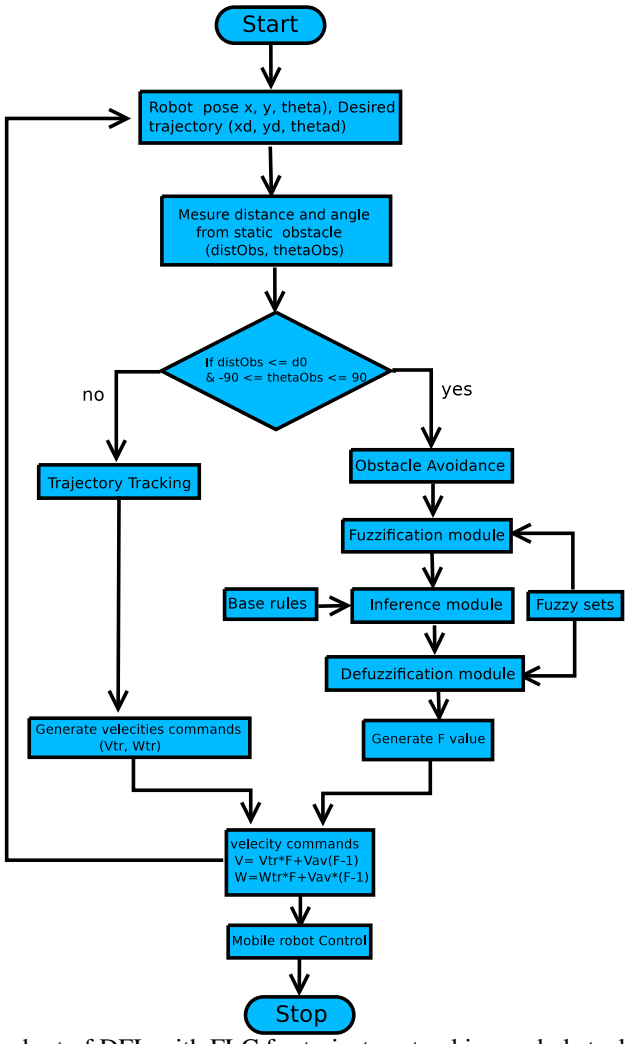

Fig. 5. Flowchart of DFL with FLC for trajectory tracking and obstacle avoidance

4. Simulation Results and Discussion

Using a TurtleBot2 mobile robot, we carried out exact computational tests to evaluate the viability and efficacy of a Dynamic Feedback Linearization (DFL) for trajectory tracking and Fuzzy Logic Controller (FLC) for obstacle avoidance. A powerful computer environment with an Intel Core i9 processor, a 12GB NVIDIA GPU, 32GB of RAM, and Linux Ubuntu 20.04 LTS was used for the research. To ensure a comprehensive assessment, we designed and compared various navigation strategies based on the proposed algorithms. The specifications and key parameters of the TurtleBot2 are summarized in Table. 4. For motion planning and control, we utilized the ROS framework, generating control signals with the TurtleBot2 and collecting sensor data, including odometry feedback.

All simulations were executed in a realistic and controlled testing environment using the 3D Gazebo simulator and MATLAB 2020b, integrated with the ROS1 Noetic middleware. This setup allowed us to achieve accurate evaluations and robust validation of the proposed approach.

4.1. Trajectory Tracking

The task of directing the mobile robot to follow a predetermined produced path was our first consideration, as shown in Fig. 6. This path serves as the reference trajectory for the tracking task and is mathematically defined in (12), where $0 \leq t \leq T$, with T representing the total execution time. The parameter a is a positive constant that remains fixed throughout the experiment.

The values of all fixed parameters utilized in the proposed tracking control algorithm are provided in Table. 2.

$$\begin{cases} x_d(t) = a * sin(t/10) \\ y_d(t) = a * sin(t/20) \end{cases} \tag{12}$$

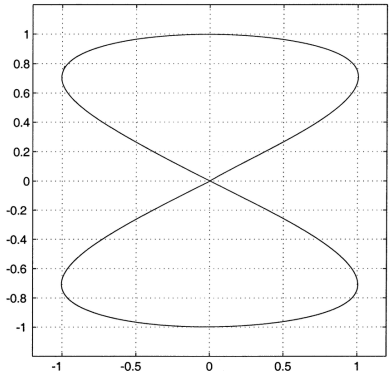

Fig. 6. Considered eight shape task [52]

Table 2. Simulation Parameters

Parameter	Value
Sampling time (dt)	0.1 (s)
Simulation time (T)	126 (s)
constant (a)	2
Linear tracking velocity (vt)	0.11 (m/s)
k_{p1}	1
k_{p2}	1
k_{d1}	0.7
k_{d2}	0.7
k_{th}	1

In this experiment, the mobile robot shown in Fig. 7 is a differential drive robot, the TurtleBot2, operating in an empty environment as depicted in Fig. 8a. The green circle represents the starting point, while the black cylindrical shape represents the mobile robot.

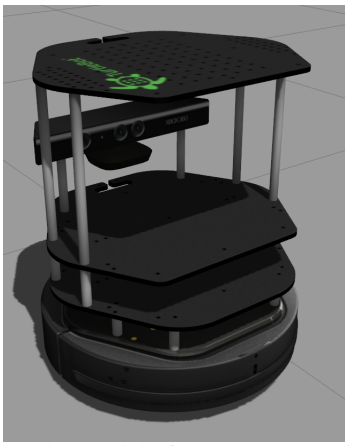

Fig. 7. Gazebo model of Turtlebot2 mobile robot

The results of applying the proposed approach are presented in Fig. 9. In Fig. 9a illustrates the tracking errors in x, y, and θ between the reference and actual trajectories during the task. The

small error values observed confirm the effectiveness of the proposed approach in achieving accurate trajectory tracking. Furthermore, In Fig. 9b shows the linear speed v and angular speed ω of the mobile robot during the task, with the blue curve representing the linear speed and the red curve representing the angular speed. The smooth variations in both velocity components indicate that the motion remains well within the robot's dynamic constraints, ensuring stable and controlled behavior.

In Fig. 10a illustrates the tracking results, where the blue curve represents the reference trajectory and the red curve shows the executed trajectory. It can be observed that the actual trajectory closely follows the reference with minimal deviation, demonstrating smooth and accurate tracking performance.

In Fig. 8b shows the trajectory tracking visualization in the ROS RViz tool. The green circle indicates the starting point, while the blue curve represents the actual trajectory of the mobile robot from the starting point to the endpoint.

The plotted results confirm the efficiency of the proposed approach, as the robot closely follows the reference trajectory with minimal deviation. The small error between the reference and actual trajectories further validates the accuracy of the method.

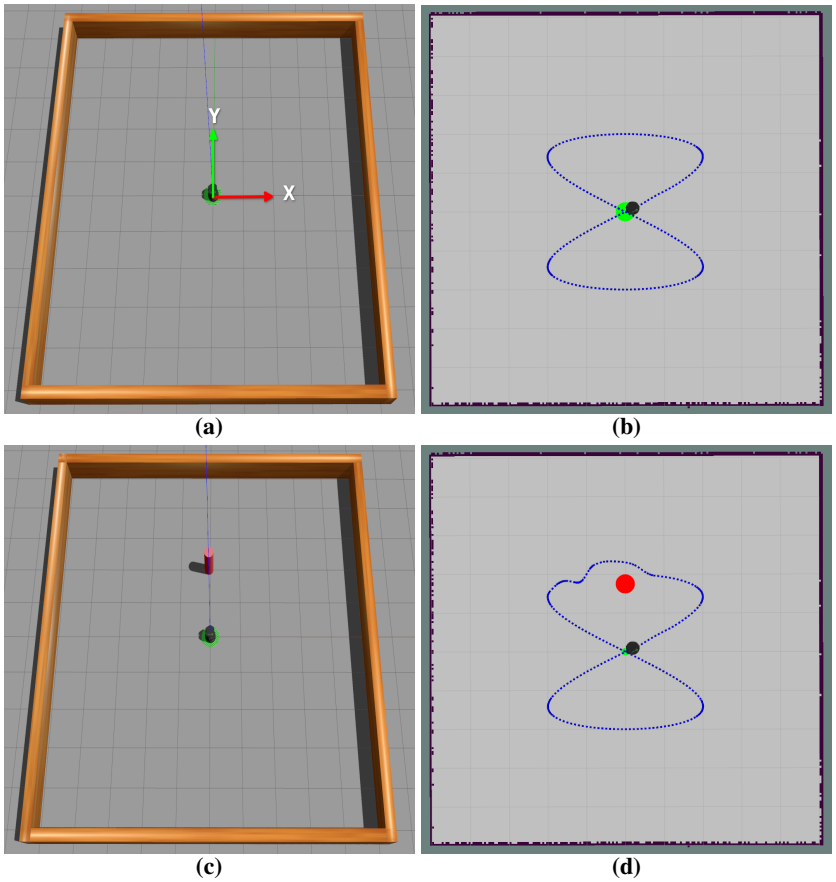

Fig. 8. Robot Environments in 3D simulator Gazebo and RViz Visualization Tool: (a) Robot environment without obstacle, (b) Visualization of the executed trajectory of the robot in the case without obstacle, (c) Robot environment with static obstacle, (d) Visualization of the executed trajectory of the robot in the case with static obstacle

4.2. Obstacle Avoidance

Secondly, a static obstacle is introduced along the predefined reference path as shown in Fig. 8.c, presents a static Gazebo environment designed for the robot's obstacle avoidance task. The green circle marks the starting point of the robot, while the red cylinder represents the static obstacle positioned

at coordinates (0,2) relative to the fixed global reference frame. This setup provides a controlled environment to test the robot's ability to move around obstacles while remaining on the desired trajectory.

In Fig. 9c and Fig. 9.d, the tracking error and the variation in speed during the trajectory tracking with obstacle avoidance behavior. It can be observed that the error remains very small during the tracking phase but increases during the obstacle avoidance task, particularly in terms of orientation, as the robot adjusts to avoid the obstacle and ensure its safety. In Fig. 9.d, we observe a small variation in the robot's speed, both linear and angular, during the tracking phase . However, there is a larger variation in speed, especially in the angular velocity, during the obstacle avoidance phase.

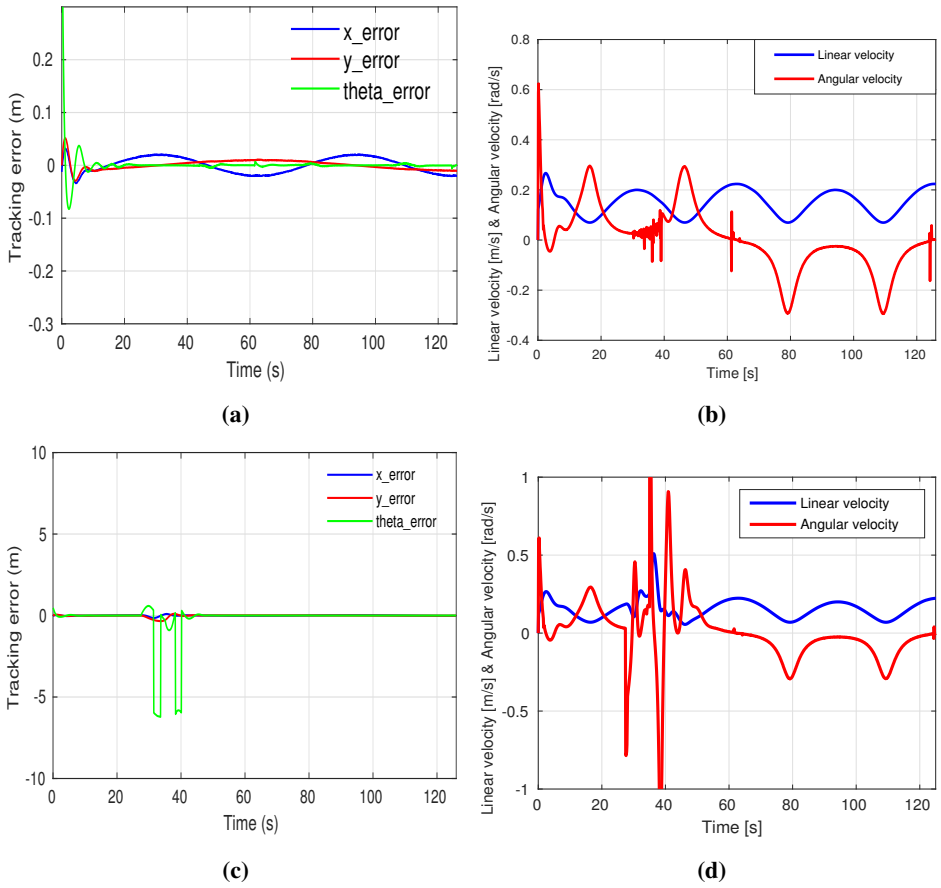

Fig. 9. Error analysis and robot velocities variation (a) Change errors in X, Y, and θ directions for trajectory tracking, (b) Linear and angular velocities of the robot during the tracking task, (c) Change errors in X, Y, and θ directions in the tracking with avoidance behavior, (d) Linear and angular velocities in tracking control with obstacle avoidance

In Fig. 10.b illustrates the tracking and avoidance results, where the blue curve represents the reference trajectory and the red curve shows the executed trajectory, black star is static and known obstacle, It can be observed that the actual trajectory closely follows the reference with minimal deviation during trajectory tracking task and higher deviation when distance between robot and obstacle less than security distance demonstrating smooth and accurate and safe tracking performance.

In Fig. 8.d shows the trajectory tracking and obstacle avoidance visualization in the ROS RViz tool. The green circle indicates the starting point, red cercle is static obstacle while the blue curve represents the actual trajectory of the mobile robot from the starting point to the endpoint.

Simulation data results of the both tasks are defined in Table. 3, The low MSE values for both

position and orientation confirm the high accuracy and efficiency of our approach in trajectory tracking. This indicates minimal deviation from the planned path, ensuring robust and precise navigation.

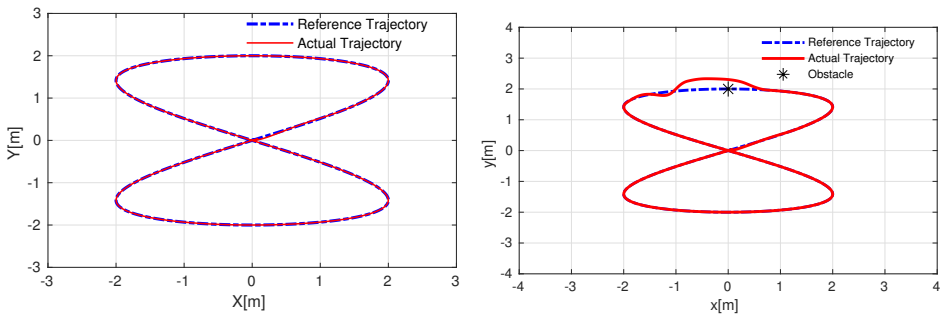

(a) **(b)**

Fig. 10. Trajectory tracking and obstacle avoidance (a) tracking process, (b) tracking with obstacle avoidance

Table 3. Simulation experiment data results

Task	Position error	Orientation error	Time (s)	Tracking accuracy (%)	OA Success rate (%)
Tracking	0.13 (MSE)	0.46 (MSE)	129	93	-
Avoidance	-	-	131	-	95

5. Experiments and Results Validation

To verify the effectiveness of the algorithms proposed in this paper, the Robot Operating System (ROS) was used for experimental validation. The experimental environment consisted of a 64-bit Ubuntu 20.04 operating system, furnished with an Intel Core i9 processor, 32 GB of RAM memory, and a 12 GB Nvidia GeForce graphics card, while the experimental platform operates on ROS Noetic, The trajectory following and obstacle avoidance tasks began at the starting point (0,0), with the target point located at the same position. The mobile robot used for testing is shown in Fig. 11.a. It is equipped with multiple sensors, including an Inertial Measurement Unit (IMU), Lidar SICK LMS200, MS Kinect v1 depth camera, 16 sonar sensors, and a wheel encoder. The robot features differential drive locomotion. The obstacle used for the obstacle avoidance task is a rectangular block 0.2 m × 0.3 m, which is placed in the field. In the experiment, a master-slave wireless connection was configured. The low-level laptop PC on the mobile robot acted as the slave, while the high-level powerful PC, running ROS, served as the master for controlling the system.

Table. 4 lists the selection of some main parameters of the mobile robots used in the simulation and experimental part. The choice of parameters effects the performance of our approach for certain extent. The parameters outlined in Table. 4 fully satisfy this study's experimental requirements. Wheel encoders, devices used to measure a robot's position and orientation, play a crucial role in kinematic modelling. They serve as fundamental parameters for the algorithm proposed in this paper. The accuracy of the encoder data significantly influences the algorithm's performance, as any inaccuracies can directly affect the precision of the tracking and avoidance behaviours.

5.1. Trajectory Following

In Fig. 11a, depicated the Adapt mobile robot Pioneer3dx DWMR is equipped with an onboard netbook PC and all the sensors required in mobile robot navigation, In Fig. 11b represents its environment, which as a square area measuring 4 m × 4 m the green square area represents the starting point. In Fig. 12a illustrating the tracking behavior in the real mobile robot, the red curve (eight shape) represents the executed trajectory from the starting point to the endpoint during the tracking task. The

motion appears smooth and accurate, as depicted in Fig. 13a using the ROS RViz tool, where the blue curve represents the actual trajectory, and the robot is centered. In Fig. 14a illustrates the tracking error during the trajectory-following task. It can be observed that the error is very small, with minor fluctuations occurring occasionally due to the robot's motion and odometer measurements.

(a) **(b)**

Fig. 11. Environmental modelling (a) Adapt Mobilerobots Pioneer 3-Dx, (b) Real environment of mobile robot

Table 4. Parameters of the two mobile robots: TurtleBot2 and Pioneer-3DX

Parameter	Turtlebot2	Pioneer-3DX
Robot weight	6.3 (kg)	9 (kg)
Operating payload	5 (kg)	17 (kg)
Max. forward/backward Speed	0.65 (m/s)	1.2 (m/s)
Rotation speed	3.14 (rad/s)	5.23 (rad/s)
Locomotion drive	Differential drive	Differential drive
Traversable terrain	Indoor	Indoor, Outdoor

In Fig. 14b shows the linear velocity (blue curve) and angular velocity (red curve). Both velocity profiles appear smooth and within acceptable limits. In Fig. 15a defined results of tracking that blue and rerepresenting the executed and reference trajectories, respectively, we can see the executed and reference are very similar. The video demonstrations are available at: https://youtu.be/CybDwajlTUU

5.2. Obstacle Avoidance

In Fig. 12.b presents the tracking process with obstacle avoidance task. The green box indicates a static obstacle that the robot successfully avoids while following the predefined path based Dynamic Feedback Linearization (DFL) approach. As shown in Fig. 13.b the visualization of the executed trajectory in the RViz tool, the blue curve indicates the actual trajectory, and the red circle presents the static obstacle, which the robot avoids during the period of time between 26-36 seconds.

In Fig. 14c illustrates the tracking error during the tracking process with avoidance behavior. It can be observed that the error is very small, with minor fluctuations occurring occasionally due to the robot's motion and odometer measurements.

In Fig. 14d shows the linear velocity (blue curve) and angular velocity (red curve). Both velocity profiles appear smooth and within acceptable limits.

In Fig. 15b defined results of tracking with avoidance that red and blue represents the executed and reference trajectories respectively we can see the executed and reference is very similar. The video demonstrations are available at: https://youtu.be/Z6Bi9SjnEjY?si=V4Erc6knmebz41R-

Simulation data results of the both tasks are defined in Table. 5, It can be seen that the small deference of the path length and traveled time for both tasks for safe navigation of mobile robot

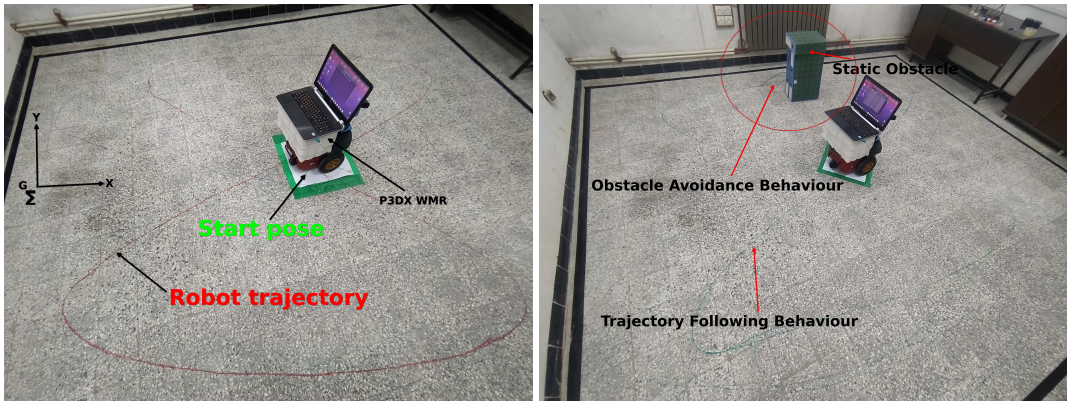

(a) (b)

Fig. 12. Trajectory tracking and Obstacle avoidance (a) tracking process, (b) tracking with obstacle avoidance

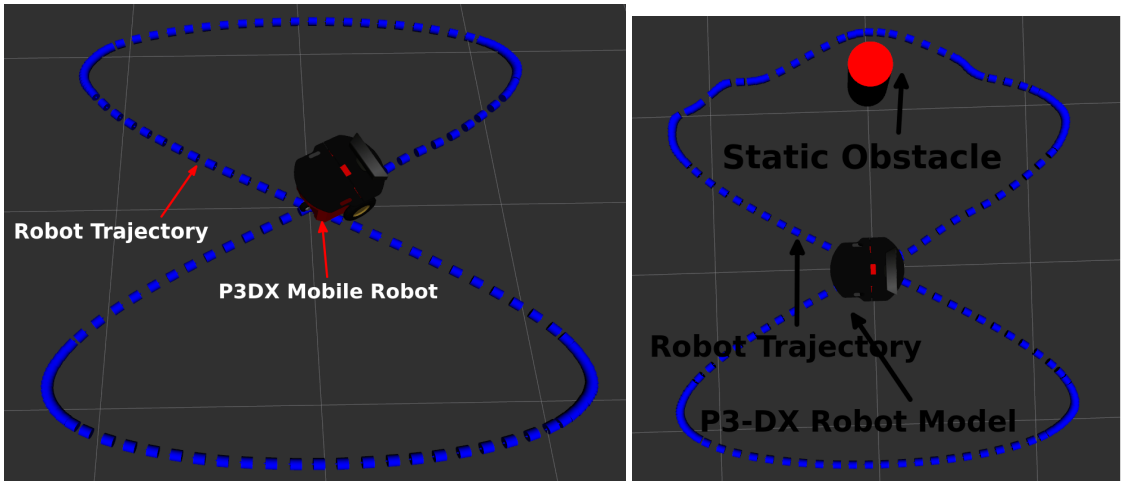

Fig. 13. Visualization trajectories by RViz tool (a) Visualization of actual trajectory in tracking task, (b) Visualization of actual trajectory in tracking with avoidance tasks

By comparing the results obtained from simulations and practical experiments conducted using the ROS middleware, it can be concluded that the proposed approach is both efficient and adaptable. The consistency between the simulation and real-world outcomes highlights the robustness and practicality of the methodology in diverse scenarios.

Table 5. Practical experiment data results

Behavior	Path length (m)	Time (s)
Trajectory tracking	11.77	123
Obstacle avoidance	12.05	126

6. Conclusion

An innovative Dynamic Feedback Linearization (DFL) control algorithm, integrated with Fuzzy Logic Control (FLC), has been proposed to tackle the complex challenges of robust trajectory tracking and obstacle avoidance for Differentially-Driven Mobile Robots (DWMRs). The approach begins by leveraging the flatness property to simplify the intertwined problems of motion planning and control design. The controller is designed in the flat output space to ensure precise trajectory tracking and maintain system stability.

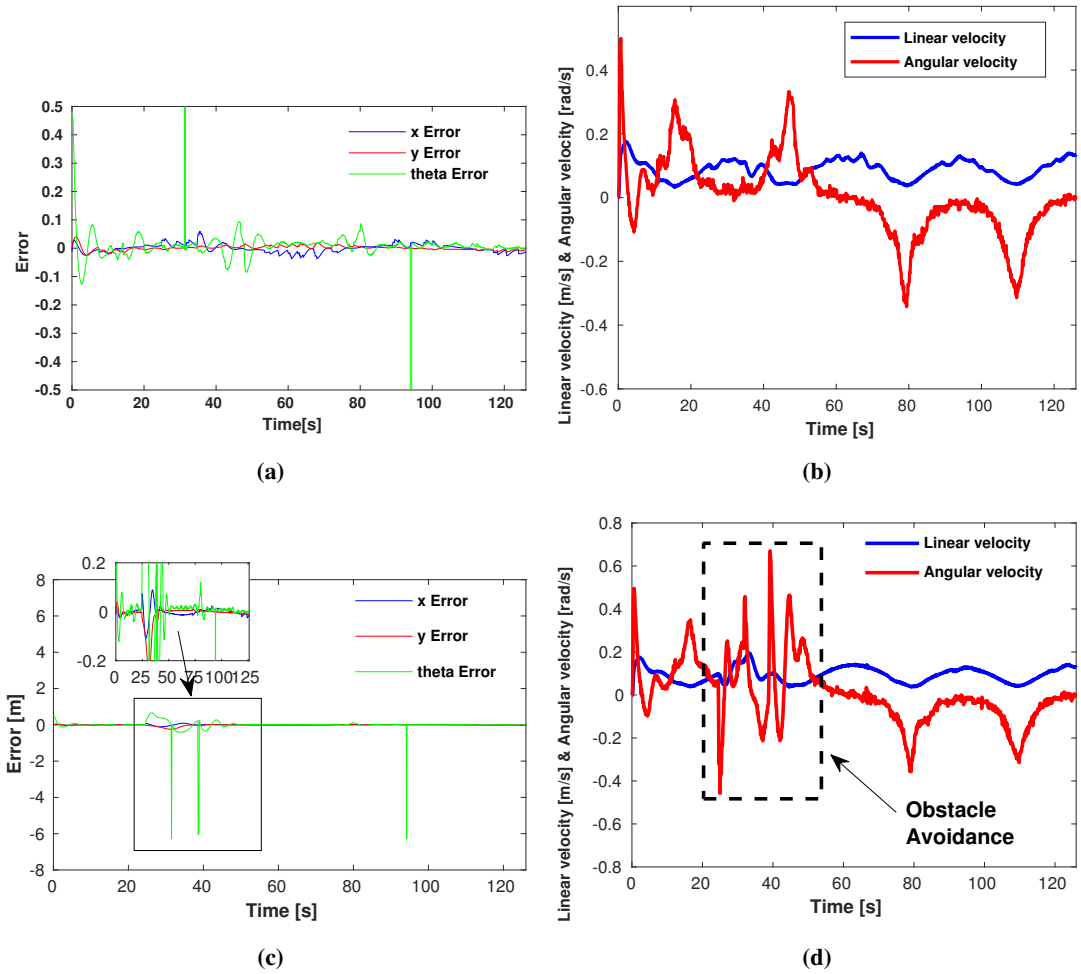

Fig. 14. Error analysis and velocities variation in trajectory tracking and obstacle avoidance tasks (a) Error changes in X, Y, and θ directions for trajectory tracking, (b) Linear and angular velocities, (c) Change errors in X, Y, and θ-direction for tracking with avoidance tasks, (d) Linear and angular velocities during tracking and avoidance behaviors

A key advantage of combining flatness-based feedback with fuzzy logic control is the significant improvement in system performance, motion accuracy, and perturbation rejection when compared to conventional linear flatness-based controllers. The proposed methodology has been rigorously validated through a combination of theoretical analysis, extensive simulations, and experimental testing. These validations consistently highlight the system's robust tracking capabilities and exceptional accuracy in obstacle avoidance across the prescribed tasks.

On the one hand, the proposed approach has certain limitations, including increased complexity and computational demands due to the combination of these two control strategies. These challenges, which are not addressed in this study, could be significant in real-time applications. Future enhancements will focus on optimizing computational efficiency and reducing complexity to improve real-time performance.

On the other hand, incorporating dynamic obstacle handling and integrating advanced sensor technologies, such as laser scanners and vision cameras, will significantly enhance the robot's environmental perception. These upgrades will enable it to navigate safely and efficiently in both static and dynamic environments. This continuous evolution will ensure that the proposed approach remains highly effective and adaptable to increasingly complex real-world scenarios.

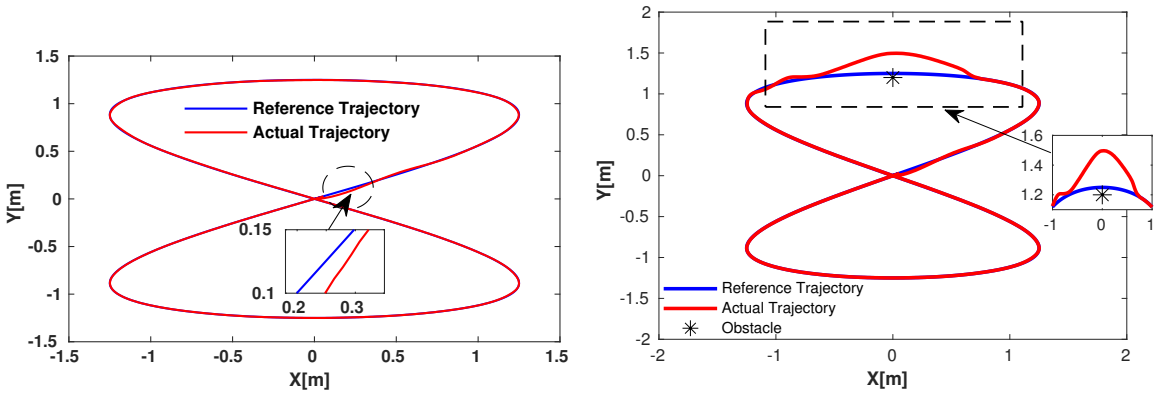

(a) (b)

Fig. 15. Error analysis in tracking without and with avoidance: (a) tracking process, (b) tracking with obstacle avoidance

Author Contribution: All authors contributed equally to the main contributor to this paper. All authors read and approved the final paper.

Data Availability Statement: The MATLAB source code and ROS integration will be available at (The code is in Progress) https://github.com/souhaiblou/Fuzzy_DynamicFeedbackLinearization_Matlab_ROS/tree/main

Funding: This research received no external funding

Acknowledgment: The authors wish to express their gratitude to the editor and reviewers for their valuable time and constructive feedback, which have significantly enhanced the quality of this paper.

Conflicts of Interest: The authors declare no conflict of interest.

List of Symbols and Abbreviations

P3DX	: Pioneer 3DX
MSE	: Mean Square Error
DWMR	: Differential Wheeled Mobile Robot
ROS	: Robot Operating System
DFL	: Dynamic Feedback Linearization
FDFL	: Fuzzy Dynamic Feedback Linearization
FLC	: Fuzzy Logic Controller
OA	: Obstacle Avoidance
q	: Robot pose
v	: Linear velocity (m/s)
ω	: Angular velocity (rad/s)
θ	: Robot heading angle (°)
ξ	: Linear acceleration

Appendix

Appendix A: Kinematic model

From (1), the linear velocity v can be written as the following:

$$v = \omega R \tag{13}$$

Where R denotes the radius of both robot wheels. Then one can get this:

$$v_R = \omega(R + \frac{L}{2}) \tag{14}$$

$$v_L = \omega(R - \frac{L}{2}) \tag{15}$$

$$R = \frac{L}{2}\,(\frac{v_R + v_L}{v_R - v_L}) \tag{16}$$

Finally, from the above demonstrations, the linear velocity can be written as

$$v = \frac{v_R + v_L}{2} \tag{17}$$

The angular velocity depends on the difference between the linear velocity of right and left velocities, respectively.

$$v_R - v_L = \omega\,(R + \frac{L}{2}) - \omega\,(R - \frac{L}{2}) \tag{18}$$

$$v_R - v_L = \omega\, L \tag{19}$$

After that, the angular velocity ω can be written as:

$$\omega = \frac{v_R - v_L}{L} \tag{20}$$

Appendix B: Flatness concept

From (24) , The kinematic model of the nominal DWMR system can be also written as [54]:

$$\ddot{F} = \; u = \begin{bmatrix} u_1 \\ u_2 \end{bmatrix} \tag{21}$$

The above equation obtained from the second derivative of flatness output F

$$F = \begin{bmatrix} F_1, F_2 \end{bmatrix}^T = \begin{bmatrix} x, y \end{bmatrix}^T \tag{22}$$

$\dot{F}$ with respect to time returns:

$$\dot{F} = \begin{bmatrix} \dot{F}_1 \\ \dot{F}_2 \end{bmatrix} = \begin{bmatrix} \dot{x} \\ \dot{y} \end{bmatrix} = v \begin{bmatrix} cos(\theta) \\ sin(\theta) \end{bmatrix} = w \begin{bmatrix} 0 \\ 0 \end{bmatrix} \tag{23}$$

$$\ddot{F} = \begin{bmatrix} \ddot{x} \\ \ddot{y} \end{bmatrix} = \begin{bmatrix} \cos(\theta) & -v\sin(\theta) \\ \sin(\theta) & v\cos(\theta) \end{bmatrix} \begin{bmatrix} \xi \\ \omega \end{bmatrix} \tag{24}$$

With ξ = $\dot{v}$.

References

[1] J. Yao and M. Xin, "Suboptimal control design for differential wheeled mobile robots with $\theta-$D technique," in *2021 60th IEEE Conference on Decision and Control (CDC)*, pp. 1444–1449, 2021, https://doi.org/10.1109/CDC45484.2021.9683480.

[2] E. A. Padilla-García, R. D. Cruz-Morales, J. González-Sierra, D. Tinoco-Varela, and M. R. Lorenzo-Gerónimo, "Design, assembly and control of a differential/omnidirectional mobile robot through additive manufacturing," *Machines*, vol. 12, no. 3, p. 163, 2024, https://doi.org/10.3390/machines12030163.

[3] H. T. Najm, N. S. Ahmad, and A. S. Al-Araji, "Enhanced path planning algorithm via hybrid WOA-PSO for differential wheeled mobile robots," *Systems Science & Control Engineering*, vol. 12, no. 1, 2024, https://doi.org/10.1080/21642583.2024.2334301.

[4] J. Kim and B. K. Kim, "Cornering trajectory planning avoiding slip for differential-wheeled mobile robots," in *IEEE Transactions on Industrial Electronics*, vol. 67, no. 8, pp. 6698–6708, 2020, https://doi.org/10.1109/TIE.2019.2941156.

[5] D. M. Vargas, V. V. Rincón, A. L. Álvarez, A. R. Castro, M. M. Cruz, and J. Rubio, "Navigation of a differential wheeled robot based on a type-2 fuzzy inference tree," *Machines*, vol. 10, no. 8, p. 660, 2022, https://doi.org/10.3390/machines10080660.

[6] M. Yao, H. Deng, X. Feng, P. Li, Y. Li, and H. Liu, "Global path planning for differential drive mobile robots based on improved BSGA* algorithm," *Applied Sciences*, vol. 13, no. 20, p. 11290, 2023, https://doi.org/10.3390/app132011290.

[7] A. Šelek, M. Seder, and I. Petrović, "Smooth autonomous patrolling for a differential-drive mobile robot in dynamic environments," *Sensors*, vol. 23, no. 17, p. 7421, 2023, https://doi.org/10.3390/s23177421.

[8] R. Mathew and S. S. Hiremath, "Development of waypoint tracking controller for differential drive mobile robot," in *2019 6th International Conference on Control, Decision and Information Technologies (CoDIT)*, pp. 1121-1126, 2019, https://doi.org/10.1109/CoDIT.2019.8820389.

[9] C.-L. Shih and L.-C. Lin, "Trajectory planning and tracking control of a differential-drive mobile robot in a picture drawing application," *Robotics*, vol. 6, no. 3, p. 17, 2017, https://doi.org/10.3390/robotics6030017.

[10] T. N. T. Cao, B. T. Pham, N. T. Nguyen, D.-L. Vu, and N.-V. Truong, "Second-order terminal sliding mode control for trajectory tracking of a differential drive robot," *Mathematics*, vol. 12, no. 17, p. 2657, 2024, https://doi.org/10.3390/math12172657.

[11] C. Wang, P. Shi, and I. Rudas, "Tracking control for two-wheeled mobile robots via event-triggered mechanism," *ISA Transactions*, vol. 156, pp. 632–638, 2025, https://doi.org/10.1016/j.isatra.2024.11.032.

[12] H. Huang and J. Gao, "Backstepping and novel sliding mode trajectory tracking controller for wheeled mobile robots," *Mathematics*, vol. 12, no. 10, p. 1458, 2024, https://doi.org/10.3390/math12101458.

[13] S. Moorthy and Y. H. Joo, "Formation control and tracking of mobile robots using distributed estimators and A biologically inspired approach," *Journal of Electrical Engineering & Technology*, vol. 18, no. 3, pp. 2231–2244, 2023, https://doi.org/10.1007/s42835-022-01213-0.

[14] H. Li and A. V. Savkin, "An algorithm for safe navigation of mobile robots by a sensor network in dynamic cluttered industrial environments," *Robotics and Computer-Integrated Manufacturing*, vol. 54, pp. 65–82, 2018, https://doi.org/10.1016/j.rcim.2018.05.008.

[15] C. Wang, J. Wang, C. Li, D. Ho, J. Cheng, T. Yan, L. Meng, M.Q.-H. Meng, "Safe and robust mobile robot navigation in uneven indoor environments," *Sensors*, vol. 19, no. 13, p. 2993, 2019, https://doi.org/10.3390/s19132993.

[16] A. N. Ouda and A. Mohamed, "Autonomous fuzzy heading control for a multi-Wheeled Combat Vehicle," *International Journal of Robotics and Control Systems*, vol. 1, no. 1, pp. 90–101, 2021, https://doi.org/10.31763/ijrcs.v1i1.286.

[17] S. Srey and S. Srang, "Adaptive controller based on estimated parameters for quadcopter trajectory tracking," *International Journal of Robotics and Control Systems*, vol. 4, no. 2, pp. 480–501, 2024, https://doi.org/10.31763/ijrcs.v4i2.1342.

[18] M. S. Qasim, A. B. Ayoub, and A. I. Abdulla, "NMPC based-trajectory tracking and obstacle avoidance for mobile robots," *International Journal of Robotics and Control Systems*, vol. 4, no. 4, pp. 2026–2040, 2024, https://doi.org/10.31763/ijrcs.v4i4.1605.

[19] Y. Raoui and N. Elmennaoui, "Accurate robot navigation using visual invariant features and dynamic neural fields," *International Journal of Robotics and Control Systems*, vol. 4, no. 4, pp. 1584–1601, 2024, https://doi.org/10.31763/ijrcs.v4i4.1545.

[20] M. M. J. Samodro, R. D. Puriyanto, and W. Caesarendra, "Artificial Potential Field path planning algorithm in differential drive mobile robot platform for dynamic environment," *International Journal of Robotics and Control Systems*, vol. 3, no. 2, pp. 161–170, 2023, https://doi.org/10.31763/ijrcs.v3i2.944.

[21] A. Abadi, A. Ayeb, M. Labbadi, D. Fofi, T. Bakir, and H. Mekki, "Robust Tracking Control of Wheeled Mobile Robot Based on Differential Flatness and Sliding Active Disturbance Rejection Control: Simulations and Experiments," *Sensors*, vol. 24, no. 9, pp. 2849, 2024, https://doi.org/10.3390/s24092849.

[22] S. Khesrani, A. Hassam, O. Boutalbi, and M. Boubezoula, "Motion planning and control of nonholonomic mobile robot using flatness and fuzzy logic concepts," *International Journal of Dynamics and Control*, vol. 9, no. 4, pp. 1660–1671, 2021, https://doi.org/10.1007/s40435-020-00754-4.

[23] H. Xie, J. Zheng, R. Chai, and H. T. Nguyen, "Robust tracking control of a differential drive wheeled mobile robot using fast nonsingular terminal sliding mode," *Computers & Electrical Engineering*, vol. 96, p. 107488, 2021, https://doi.org/10.1016/j.compeleceng.2021.107488.

[24] Z. Sun, H. Xie, J. Zheng, Z. Man, and D. He, "Path-following control of Mecanum-wheels omnidirectional mobile robots using nonsingular terminal sliding model," *Mechanical Systems and Signal Processing*, vol. 147, no. 107128, p. 107128, 2021, https://doi.org/10.1016/j.ymssp.2020.107128.

[25] Y. Xie *et al.*, "Coupled fractional-order sliding mode control and obstacle avoidance of a four-wheeled steerable mobile robot," *ISA Transactions*, vol. 108, pp. 282–294, 2021, https://doi.org/10.1016/j.isatra.2020.08.025.

[26] A. Haqshenas M., M. M. Fateh, and S. M. Ahmadi, "Adaptive control of electrically-driven nonholonomic wheeled mobile robots: Taylor series-based approach with guaranteed asymptotic stability," *International Journal of Adaptive Control and Signal Processing*, vol. 34, no. 5, pp. 638–661, 2020, https://doi.org/10.1002/acs.3104.

[27] R. Miranda-Colorado and N. R. Cazarez-Castro, "Observer-based fuzzy trajectory-tracking controller for wheeled mobile robots with kinematic disturbances," *Engineering Applications of Artificial Intelligence*, vol. 133, p. 108279, 2024, https://doi.org/10.1016/j.engappai.2024.108279.

[28] R. Kubo, Y. Fujii, and H. Nakamura, "Control lyapunov function design for trajectory tracking problems of wheeled mobile robot," *IFAC-PapersOnLine*, vol. 53, no. 2, pp. 6177–6182, 2020, https://doi.org/10.1016/j.ifacol.2020.12.1704.

[29] Z. Tao, Y.-H. Wang, G.-Q. Li, and G. Hou, "Lyapunov based global trajectory tracking control of wheeled mobile robot," *Journal of Physics: Conference Series*, vol. 2478, no. 10, p. 102018, 2023, https://doi.org/10.1088/1742-6596/2478/10/102018.

[30] G. Oriolo, A. De Luca, and M. Vendittelli, "WMR control via dynamic feedback linearization: design, implementation, and experimental validation," in *IEEE Transactions on Control Systems Technology*, vol. 10, no. 6, pp. 835–852, 2002, https://doi.org/10.1109/TCST.2002.804116.

[31] L. Martins, C. Cardeira, and P. Oliveira, "Feedback linearization with zero dynamics stabilization for quadrotor control," *Journal of Intelligent & Robotic Systems*, vol. 101, no. 7, 2021, https://doi.org/10.1007/s10846-020-01265-2.

[32] H. Xie, J. Zheng, Z. Sun, H. Wang, and R. Chai, "Finite-time tracking control for nonholonomic wheeled mobile robot using adaptive fast nonsingular terminal sliding mode," *Nonlinear Dynamics*, vol. 110, no. 2, pp. 1437–1453, 2022, https://doi.org/10.1007/s11071-022-07682-2.

[33] A. Keymasi Khalaji and M. Jalalnezhad, "Robust forward-backward control of wheeled mobile robots," *ISA Transactions*, vol. 115, pp. 32–45, 2021, https://doi.org/10.1016/j.isatra.2021.01.016.

[34] G. Oriolo, "Wheeled Robots," in *Encyclopedia of Systems and Control*, pp. 1–8, 2020, https://doi.org/10.1007/978-1-4471-5102-9_178-2.

[35] L. Chen and Y. Jia, "Output feedback tracking control of flat systems via exact feedforward linearization and LPV techniques," *International Journal of Control, Automation and Systems*, vol. 17, no. 3, pp. 606–616, 2019, https://doi.org/10.1007/s12555-018-0459-1.

[36] A. M. Kopp, L. Fuchs, and C. Ament, "Flatness-based identification of nonlinear dynamics", in *2024 32nd Mediterranean Conference on Control and Automation (MED)*, 2024, https://doi.org/10.1109/MED61351.2024.10566206.

[37] A. Abadi, A. E. Amraoui, H. Mekki, and N. Ramdani, "Flatness-based active disturbance rejection control for a wheeled mobile robot subject to slips and external environmental disturbances," *IFAC-PapersOnLine*, vol. 53, no. 2, pp. 9571–9576, 2020, https://doi.org/10.1016/j.ifacol.2020.12.2443.

[38] N. An, Q. Wang, X. Zhao, and Q. Wang, "Differential flatness-based distributed control of underactuated robot swarms," *Applied Mathematics and Mechanics*, vol. 44, no. 10, pp. 1777–1790, 2023, https://doi.org/10.1007/s10483-023-3040-8.

[39] K. Kaaniche, O. El-Hamrawy, N. Rashid, M. Albekairi, and H. Mekki, "Mobile robot control based on 3D visual servoing: A new approach combining pose estimation by neural network and differential flatness," *Applied Sciences*, vol. 12, no. 12, p. 6167, 2022, https://doi.org/10.3390/app12126167.

[40] J.-C. Ryu and S. K. Agrawal, "Differential flatness-based robust control of mobile robots in the presence of slip," *The International Journal of Robotics Research*, vol. 30, no. 4, pp. 463–475, 2011, https://doi.org/10.1177/0278364910385586.

[41] S. R. Sahoo and S. S. Chiddarwar, "Mobile robot control using bond graph and flatness based approach," *Procedia Computer Science*, vol. 133, pp. 213–221, 2018, https://doi.org/10.1016/j.procs.2018.07.026.

[42] K. S. Yakovlev, A. A. Andreychuk, J. S. Belinskaya, and D. A. Makarov, "Safe interval path planning and flatness-based control for navigation of a mobile robot among static and dynamic obstacles," *Automation and Remote Control*, vol. 83, no. 6, pp. 903–918, 2022, https://doi.org/10.1134/S000511792206008X.

[43] G. Rigatos, J. Pomares, P. Siano, M. AL-Numay, M. Abbaszadeh, and G. Cuccurullo, "Flatness-based control in successive loops for mechatronic motion transmission systems," *Asian Journal of Control*, vol. 26, no. 6, pp. 2807–2842, 2024, https://doi.org/10.1002/asjc.3378.

[44] K. Katona, H. A. Neamah, and P. Korondi, "Obstacle avoidance and path planning methods for autonomous navigation of mobile robot," *Sensors*, vol. 24, no. 11, p. 3573, 2024, https://doi.org/10.3390/s24113573.

[45] X. Cheng, S. Zhang, S. Cheng, Q. Xia, and J. Zhang, "Path-following and obstacle avoidance control of nonholonomic wheeled mobile robot based on deep reinforcement learning," *Applied Sciences*, vol. 12, no. 14, p. 6874, 2022, https://doi.org/10.3390/app12146874.

[46] K. K. A. Farag, H. H. Shehata, and H. M. El-Batsh, "Mobile robot obstacle avoidance based on neural network with a standardization technique," *Journal of Robotics*, vol. 2021, pp. 1–14, 2021, https://doi.org/10.1155/2021/1129872.

[47] W. Zhang, G. Xu, Y. Song, and Y. Wang, "An obstacle avoidance strategy for complex obstacles based on artificial potential field method," *Journal of Field Robotics*, vol. 40, no. 5, pp. 1231–1244, 2023, https://doi.org/10.1002/rob.22183.

[48] Y. Cao and N. Mohamad Nor, "An improved dynamic window approach algorithm for dynamic obstacle avoidance in mobile robot formation," *Decision Analytics Journal*, vol. 11, p. 100471, 2024, https://doi.org/10.1016/j.dajour.2024.100471.

[49] J. Wu, X. Ma, T. Peng, and H. Wang, "An improved Timed Elastic Band (TEB) algorithm of autonomous ground vehicle (AGV) in complex environment," *Sensors*, vol. 21, no. 24, p. 8312, 2021, https://doi.org/10.3390/s21248312.

[50] S. S. Bolbhat, A. S. Bhosale, G. Sakthivel, D. Saravanakumar, R. Sivakumar, and J. Lakshmipathi, "Intelligent obstacle avoiding AGV using vector field histogram and supervisory control," *Journal of Physics: Conference Series*, vol. 1716, no. 1, p. 012030, 2020, https://doi.org/10.1088/1742-6596/1716/1/012030.

[51] M. Al-Mallah, M. Ali, and M. Al-Khawaldeh, "Obstacles avoidance for mobile robot using Type-2 fuzzy logic controller," *Robotics*, vol. 11, no. 6, p. 130, 2022, https://doi.org/10.3390/robotics11060130.

[52] G. Oriolo, A. De Luca and M. Vendittelli, "WMR control via dynamic feedback linearization: design, implementation, and experimental validation," in *IEEE Transactions on Control Systems Technology*, vol. 10, no. 6, pp. 835-852, 2002, https://doi.org/10.1109/TCST.2002.804116.

[53] O. Boutalbi, K. Benmahammed, K. Henni, and B. Boukezata, "A high-performance control algorithm based on a curvature-dependent decoupled planning approach and flatness concepts for non-holonomic mobile robots," *Intelligent Service Robotics*, vol. 12, no. 2, pp. 181–196, 2019, https://doi.org/10.1007/s11370-018-00270-7.

[54] M. Boubezoula, A. Hassam, and O. Boutalbi, "Robust-flatness controller design for a differentially driven wheeled mobile robot," *International Journal of Control, Automation and Systems*, vol. 16, no. 4, pp. 1895–1904, 2018, http://dx.doi.org/10.1007/s12555-017-0408-4.

[55] P. S. Trakas, S. I. Anogiatis, and C. P. Bechlioulis, "Trajectory tracking with obstacle avoidance for nonholonomic mobile robots with Diamond-shaped velocity constraints and output performance specifications," *Sensors*, vol. 24, no. 14, p. 4636, 2024, https://doi.org/10.3390/s24144636.

[56] K. Zheng, "Autonomous obstacle avoidance and trajectory planning for mobile robot based on dual-loop trajectory tracking control and improved artificial potential field method," *Actuators*, vol. 13, no. 1, p. 37, 2024, https://doi.org/10.3390/act13010037.

[57] V. Sezer, "An optimized path tracking approach considering obstacle avoidance and comfort," *Journal of Intelligent & Robotic Systems*, vol. 105, no. 1, 2022, https://doi.org/10.1007/s10846-022-01636-x.

[58] M. Abdelwahab, V. Parque, A. M. R. Fath Elbab, A. A. Abouelsoud, and S. Sugano, "Trajectory tracking of wheeled mobile robots using Z-number based fuzzy logic," *IEEE Access*, vol. 8, pp. 18426–18441, 2020, https://doi.org/10.1109/ACCESS.2020.2968421.

[59] I. A. Kheioon, R. Al-Sabur, and A.-N. Sharkawy, "Design and modeling of an intelligent robotic gripper using a cam mechanism with position and force control using an adaptive neuro-fuzzy computing technique," *Automation*, vol. 6, no. 1, p. 4, 2025, https://doi.org/10.3390/automation6010004.

[60] Z. Razzaq, N. Brahimi, H. Z. U. Rehman, and Z. H. Khan, "Intelligent control system for brain-controlled mobile robot using self-learning neuro-fuzzy approach," *Sensors*, vol. 24, no. 18, p. 5875, 2024, https://doi.org/10.3390/s24185875.